

Microchannel molding: A soft lithography-inspired approach to micrometer-scale patterning

Christopher R. Martin and Ilhan A. Aksay^{a)}

Department of Chemical Engineering, Princeton University Princeton, New Jersey 08544-5263

(Received 17 February 2005; accepted 4 April 2005)

A new patterning technique for the deposition of sol-gels and chemical solution precursors was developed to address some of the limitations of soft lithography approaches. When using micromolding in capillaries to pattern precursors that exhibit large amounts of shrinkage during drying, topographical distortions develop. In place of patterning the elastomeric mold, the network of capillary channels was patterned directly into the substrate surface and an elastomer membrane is used to complete the channels. When the wetting properties of the substrate surfaces were carefully controlled using self-assembled monolayers (SAMs), lead zirconate titanate thin films with nearly rectangular cross-sections were successfully patterned. This technique, called microchannel molding (μ CM), also provided a method for aligning multiple layers such as bottom electrodes for device fabrication.

I. INTRODUCTION

Soft lithography¹ has proved to be a popular tool among researchers in search of a low-cost means to pattern thin films of polymers, metals, and ceramics. The common feature of this class of techniques is the use of an elastomeric material, most commonly polydimethylsiloxane (PDMS), with a patterned surface. The PDMS can be used either as a mold to impart patterns via physical confinement of a fluid precursor that dries to form the final structured thin film or as a stamp to directly transfer the material to the target substrate. The confinement-based techniques include microtransfer molding (μ TM),²⁻⁴ micromolding in capillaries (MIMIC),⁵⁻¹⁴ and embossing,⁹⁻¹⁸ while microcontact printing (μ CP)¹⁹⁻²⁸ is an example of stamping. Schematic drawings of these techniques are provided in Fig. 1.^{29,30}

To date, the soft lithography techniques have met with much greater success with polymeric and metallic thin films than they have with ceramic materials.²⁹ The deposition of ceramics requires the use of a liquid precursor, typically in the form of a sol or colloidal suspension. These precursors contain a large amount of aqueous and organic material that must be removed during the conversion to a dense, solid phase. A considerable amount of shrinkage occurs during drying and sintering, during which time the contours of the thin film may deviate from the original shape of the mold.¹³

For instance, the use of MIMIC to pattern thin films derived from sol-gels results in the formation of a final sintered topography in which the material has a greater thickness at the lateral edges than in the middle, as shown in the scanning electron microscope (SEM) images in Fig. 2.¹³ This defect, referred to as the “double-peak” topographical profile, can cause problems when the patterned thin film is used in the fabrication of hierarchical structures requiring pattern alignment for successive depositions of additional layers.¹³ In many microelectromechanical systems (MEMS) applications, such as microcantilever beams and resonators, control over the cross-sectional shape of the patterned thin film is desired to maintain the fidelity of the resonance modes.

The double-peak topography is the result of two effects that work in concert with each other. The PDMS mold is permeable to organic and water vapor permitting the liquid precursor to dry with the confines of the mold. When using a mold with a rectangular cross-section, the rate of evaporation of the organic and water vapor is fastest at the corners due to the higher surface-area-to-volume ratio. As a result, the film locally gels first and becomes most rigid at the corners. However, a wetting fluid preferentially adheres to regions of small radii of curvature. Thus, the drying film has not yet detached from the corner of the mold at gelation, resulting in the shape of the corners to be preserved in the final dried and sintered patterns.¹³

One solution to the problem of the double-peak topography is to eliminate the presence of sharp corners in the PDMS mold. Using rounded corners decreases the increased rate of evaporation at the corners and produces

^{a)}Address all correspondence to this author.

e-mail: iaksay@Princeton.edu

DOI: 10.1557/JMR.2005.0251

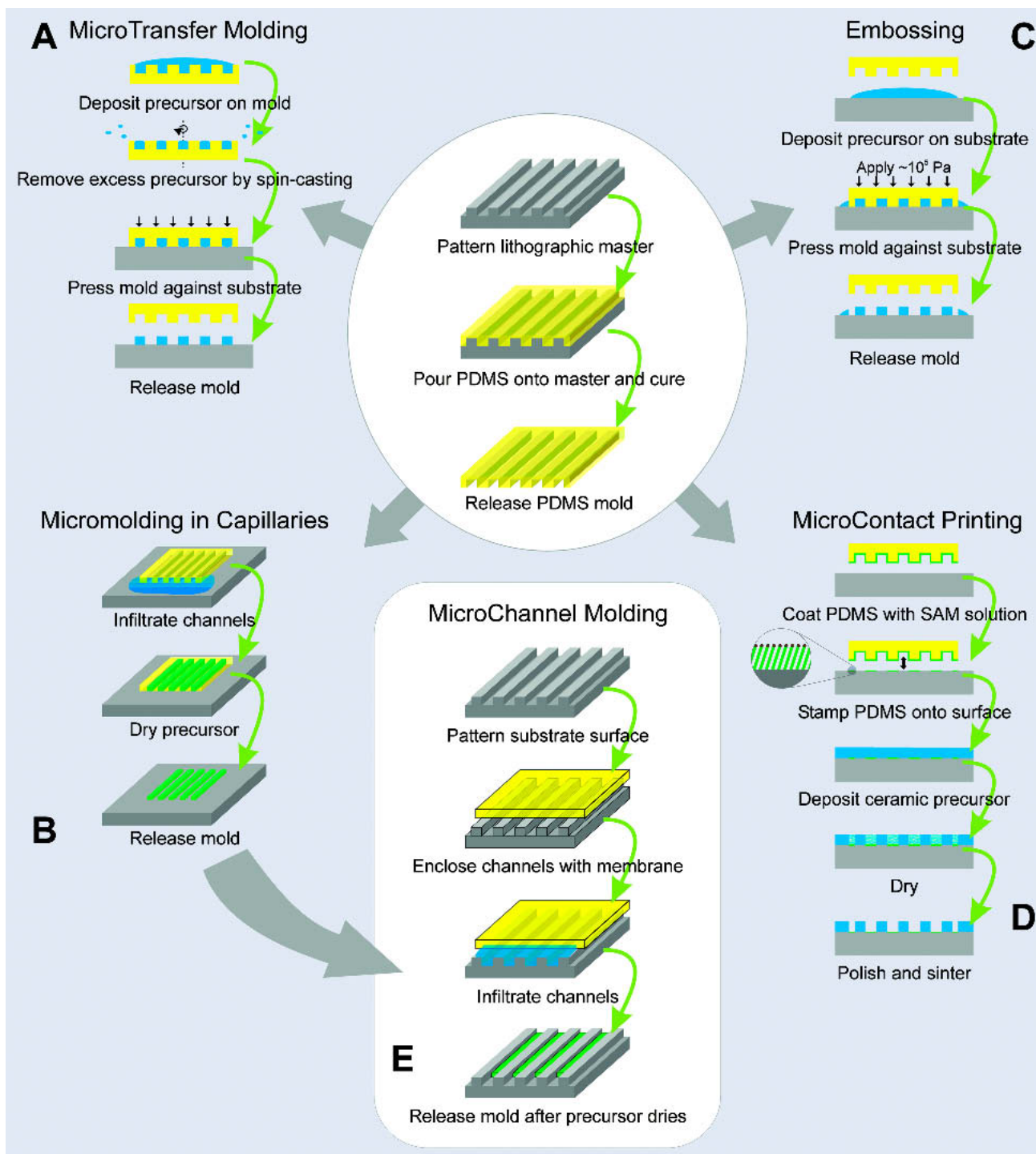


FIG. 1. Schematic illustration of PDMS mold preparation and soft lithography techniques used to pattern ceramic materials: (A) μ TM, (B) MIMIC, (C) embossing, and (D) microcontact printing (after Martin and Aksay²⁹). (E) Microchannel molding uses the same capillary filling principle as MIMIC, whereby a pool of liquid precursor is placed at the entrance region of channels formed by the patterned substrate and a flat PDMS membrane. After the fluid is drawn into the channels by capillary suction, it dries and the membrane can be peeled off. Precursor solutions such as our PZT sol-gel require a heat-treatment step to convert the gel into the desired crystal structure.

patterned thin films that better replicate the shape of the mold.¹³ However, this solution does not permit the ability to pattern thin films whose cross-section has sharp corners.

A second limitation of soft lithography techniques is the difficulty of pattern registry with the PDMS molds in the fabrication of multilayered patterned structures.³¹ As a result, the use of soft lithography to pattern thin films

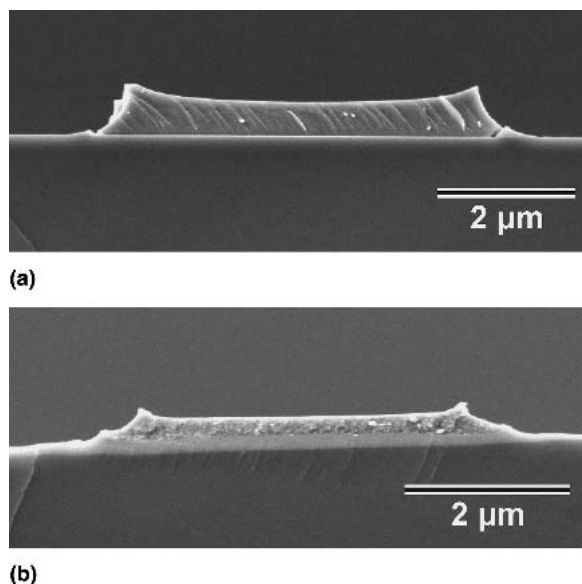


FIG. 2. SEM images of 7 μm wide lead zirconate titanate lines patterned by MIMIC with channels with 1.85 μm depth (a) after drying and (b) after heat treatment. Note the formation of the double-peaked topographical profile. Note that since a barrier layer was not used between the PZT line and the silicon substrate, an intermediate reaction layer is formed at the interface.

has yet to yield many noteworthy working devices. One example is Heule and Gauckler's use of MIMIC to pattern tin oxide in a gas sensor.¹⁴ The lack of ability to precisely register the patterned tin oxide required a fabrication scheme that allowed for a fair amount of flexibility in the placement of the electrodes and heating elements.

Using the principles of soft lithography as inspiration, we demonstrate a new technique called microchannel molding (μCM) [Fig. 1(E)]. μCM modifies MIMIC with the aim of eliminating the double-peak topographical defect while maintaining the ability to pattern features with a rectangular cross-section. Instead of using a previously patterned PDMS mold as in MIMIC, μCM requires the network of capillary channels to be directly etched into the substrate. By converting the patterned relief features of the mold to the substrate, the channel sidewalls are now impermeable to evaporation of the sol-gel during drying. The ability to pattern to submicrometer resolutions at relatively low cost is retained, while shapes are produced that more faithfully reproduce the original contours of the starting mold. With an additional processing step, the technique permits the ability to simultaneously pattern a bottom electrode contact with the patterned thin film, a convenient partial solution to the registry issue.

II. EXPERIMENTAL

A. Sol-gel preparation

The chelation-based modified sol-gel approach developed by Yi et al.³² was used to prepare the lead zirconate

titanate [$\text{Pb}(\text{Zr}_{0.52}\text{Ti}_{0.48})\text{O}_3$; PZT] chemical precursor solutions. Lead (II) acetate trihydrate (Aldrich, Milwaukee, WI) was dissolved in glacial acetic acid in a 2:1 mass ratio. The solution was heated to 105 $^\circ\text{C}$ for 5–10 min to evaporate the water from the lead acetate trihydrate. The solution was transferred to a humidity-free glove box for the addition of stoichiometric amounts of zirconium (IV) propoxide and titanium (IV) isopropoxide (both supplied by Aldrich). The solution was stirred for about 10 min after the addition of each metal alkoxide. Next, the solution was removed from the glove box, and distilled water was added to initiate the condensation reactions and promote the formation of the metal-oxide oligomeric chains. The amount of water addition can be used to adjust the viscosity, but this also impacts the amount of volumetric shrinkage of the sol-gel upon drying and heat treatment. Water was added in a 1:2 mass ratio to the initial amount of lead acetate trihydrate.

B. Substrate preparation

Patterned (100) Si wafers (SiliconQuest International, Santa Clara, CA) were used as the substrate with impermeable sidewalls. The surface of the wafer was cleaned by a piranha cleaning procedure using a 7:3 volume ratio of concentrated sulfuric acid to 30% hydrogen peroxide. The wafer was submerged in the piranha solution for 10 min at 100 $^\circ\text{C}$, then rinsed with distilled wafer, and blown dry with filtered nitrogen gas. The channels were patterned by a chrome photomask (Adtek Photomask, Montreal, QC, Canada) whose design produced linear channels with widths of 2, 3, 5, 7, 10, 15, and 20 μm in close proximity to each other. Photolithography was used to transfer the pattern into a 1.4 μm thick layer of photoresist (Clariant AZ-5214, Somerville, NJ) spin-coated onto the wafer at 4000 RPM for 40 s. The photoresist then served as the mask for reactive ion etching (RIE; PlasmaTherm 720 RIE, Uniaxis USA, Inc., St. Petersburg, FL) of the channels in the silicon.

One advantage of directly etching the channels into the substrate was the ability to immediately deposit a layer on the bottom of the channels. The photoresist layer still in place after the RIE step to form the channels presents a convenient opportunity to pattern metals via lift-off to serve as a bottom electrode along the length of the channel. This self-aligning feature was demonstrated by the electron beam evaporation (Denton DV-502A E-Beam Evaporator, Moorestown, NJ) of metallic films consisting of 15 nm Ti and 70 nm Pt and then the lift-off of the material deposited outside of the channels by immersing the sample in acetone under ultrasonic agitation to dissolve the photoresist.

The wetting properties of the sol-gel on the substrates were tailored by the use of self-assembled monolayer (SAM) of octadecyltrichlorosilane (OTS) on the silicon surfaces. The hydroxyl groups from the native silicon

oxide layer were exchanged with the OTS chains to render the surface more hydrophobic. The sample was immersed in a solution of OTS in 70% hexadecane and 30% chloroform (by volume) for 1 h and then baked on a hot plate for 6 h at 120 °C. The OTS-treated surface had sol-gel wetting properties that matched that of PDMS. Goniometer measurements revealed that the wetting angle of the PZT sol-gel on the OTS-modified surface was 47°, nearly identical to the 48° angle measured on a PDMS membrane. By comparison, the sol-gel wets the native oxide layer on a silicon wafer with a much greater affinity, as evidenced by a 23° contact angle. The contact angle on Pt-coated silicon was also measured to be 23°.

C. μ CM

Figure 1(E) depicts the sequence of steps for the μ CM of the sol-gel into the channels of the patterned substrate. First, a flat PDMS membrane was placed over the top of the patterned substrate to complete the network of capillary channels. The PDMS membrane was cast against a clean, bare silicon wafer with a native oxide layer using the commercially available Sylgard 184 kit (Dow Corning, Midland, MI). The liquid prepolymer was mixed in a 10:1 ratio with the initiator and poured on top of the master. The curing polymer was held under vacuum to remove any bubbles introduced during mixing prior to being placed in an 80 °C oven overnight.

Strips of the PDMS membrane were cut using a razor blade and peeled off. They were then placed over the tops of the etched silicon channels to be filled with the sol-gel material. The ends of the channels were left exposed to serve as the entrance region where a pool of the sol-gel was placed. The sol-gel was spontaneously drawn into the channels by capillary forces. PDMS is an excellent choice of membrane material for μ CM due to its low surface energy ($\gamma_{\text{PDMS-air}} = 0.0216 \text{ N/m}$), lack of reactivity with the PZT sol-gel, and its permeability to air and water vapor.¹ These features permit the PZT gel to dry within the confines of the mold and adhere strongly to the Si surface but not to the PDMS channel walls.

To maximize the distance that the PZT sol-gel penetrates the channels, the rate of gelation and drying was reduced to 1–2 days by sealing the sample inside of Petri dishes. The humidity inside the sealed container was higher due to the lack of exchange with the laboratory air, resulting in a slower rate of evaporation. With this approach, the sol-gel infiltrated lengths of 5–10 mm into the channels, consistent with the infiltration distances observed using MIMIC.¹² Once the gel is dry, the excess material around the periphery of the mold can be scraped off with a razor blade, and the PDMS membrane is peeled off of the substrate.

μ CM and MIMIC share the same procedure of placing a pool of sol-gel precursor at the entrance region of the

network of capillary channels and using capillary forces to fill the channels. The difference between the two techniques is how the network of capillary channels is defined in the substrate preparation steps. In MIMIC the relief features are patterned into the PDMS mold which is then placed on a flat substrate, while μ CM requires the channels to be directly etched into the substrate. This change eliminates one of the two root causes of the double-peak topographical profile, the accelerated rate of evaporation at the corners.

D. Heat treatment

After removal of the PDMS membrane (in the case of μ CM samples), the patterned PZT gel is heat treated in an electric resistance furnace (Thermolyne Type 47900 Furnace, Dubuque, IA) at 600 °C for 3 h. The samples are heated using a constant ramp rate of 10 °C/min. The heat treatment permits the volatilization of any remaining organic components of the gel, densification of the film, and conversion to the crystalline perovskite phase.¹²

E. Characterization

The samples were examined with a field emission SEM (Philips XL30, FEI, Hillsboro, OR). The SEM samples were prepared by coating 2 nm iridium and examined at 5 to 10 keV. The topography of the samples was characterized by cleaving the samples with a diamond-tipped scribe and mounting them for viewing in cross-section.

III. RESULTS AND DISCUSSION

To demonstrate the μ CM concept, SEM images of sintered PZT lines patterned on Si by μ CM are shown in Fig. 3. This network of patterned PZT lines was patterned within the confines of channels of rectangular cross-section etched in silicon by RIE. While functional devices with PZT require integrated electrodes, this model system demonstrates the key principles of the new patterning technique. The wetting properties of the surface of the channels were modified by OTS to increase the contact angle of the PZT to the sidewalls. The OTS coating also allows the PZT to debond from all surfaces with the same affinity during drying and sintering. As a result, the patterned thin film is free to shrink in all directions with the same magnitude, and there is negligible buildup of stress in the lateral direction. The total shrinkage results in a final sintered volume of 18% of the original sol-gel.¹³ The resulting patterned thin film remarkably reproduces the original contours of the starting channel with very high fidelity. This film does not have the double-peak topography of the thin film patterned by MIMIC as shown in Fig. 2.

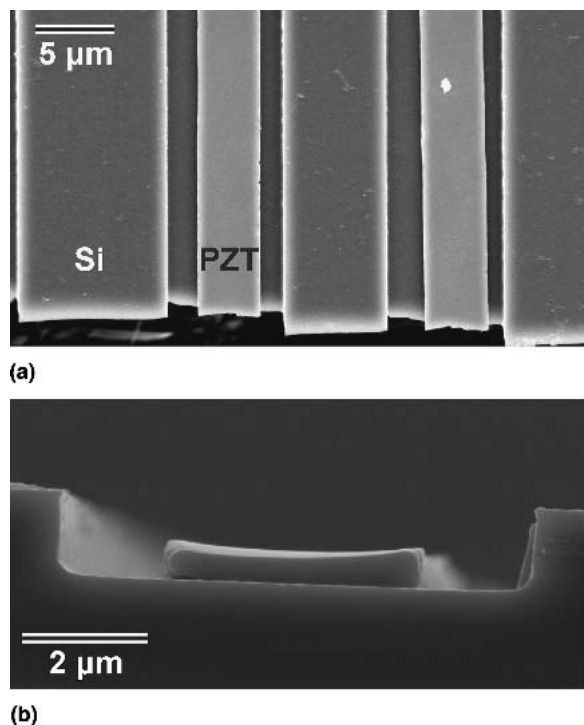


FIG. 3. SEM images of PZT patterned in OTS-treated rectangular channels (a) as seen by top view and (b) in cross section. Due to the use of the SAM-modified silicon surfaces, the formation of the intermediate layer between PZT and Si is minimized.

The role that the wetting properties play on the resulting topography of the patterned thin film is illustrated by repeating μ CM in rectangular cross-sectioned geometries without OTS coverage of the silicon surfaces. The shape of the rectangular channel, coupled with the acute wetting angle of PZT to the silicon sidewalls resulted in a meniscus-like shape to the dried PZT line [Fig. 4(a)]. This shape has an excess of material deposited at the edges and sidewalls compared to the middle of the patterned thin film. During heat treatment, this excess material is pulled laterally inward by the capillary forces that cause shrinkage, resulting in the curled profile. Interestingly, the shape of the bottom corners is preserved in the final sintered thin film [Fig. 4(b)].

The shape of the curled PZT line is distinct from the double peak topography resulting from MIMIC, shown in Fig. 2(b). The double peak topographical profile continuously evolves over the course of the drying and sintering process. The bottom surface of the PZT lines is pinned to the silicon surface as a result of the chemical reaction between PZT and the native oxide of silicon while the edges are unbound, resulting in the angled sidewalls of the thin film as the film shrinks. Conversely, the curling phenomenon principally occurs during the heat treatment of the thin film in μ CM. The PZT lines attempt to stay bound to the Si sidewalls, resisting the same lateral shrinkage force. During heat treatment, enough

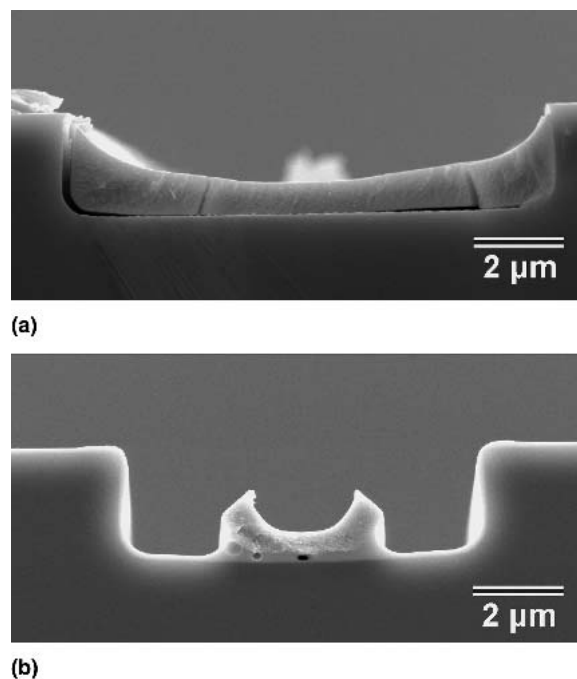


FIG. 4. SEM images of PZT patterned by μ CM in rectangular channels formed by RIE in Si without any SAM treatment (a) after drying and (b) after heat treatment. Note the formation of an interfacial layer between the PZT and Si during heat treatment.

stress builds up until a critical point is reached when the edges debond from the corners of the channel, resulting in the curled geometry.

The major disadvantage of the use of the SAM-modified surface is the loss of control over the absolute lateral dimension of the thin film. In MIMIC, the bottom corners of the patterned thin film stay pinned during both drying and heat treatment to the position where the PDMS mold contacted the substrate. By reducing the wetting affinity of the sol-gel to the surface, the shrinking thin film gains the ability to slide over the surface. The cost of this newfound ability to preserve the shape of the original channel is the inability to precisely fix the width of the patterned line. However, with prior knowledge of how much shrinkage a film will undergo, this effect can be accounted for when designing a complete hierarchical manufacturing process.

It is important to note that during heat treatment, the majority of the carbon-based SAM is pyrolyzed to produce a carbonaceous reaction barrier between the patterned line and the silicon substrate. X-ray photoelectron spectroscopy and thermogravimetric analysis studies have shown that some of the residual carbon incorporates into the growing silicon oxide layer of the substrate.³³ Although the exact mechanisms have not been determined, the deposited OTS monolayer and its residue after the pyrolysis provide a reaction barrier, preserving the structural integrity of the deposited material for later

processing steps in the fabrication of a working device or circuit. However, the improved topographical control of the patterned thin films comes at a cost. The lower force of adhesion of the PZT to the OTS-treated surface prior to heat treatment does increase the frequency of accidental delamination of the dried PZT lines when peeling off the PDMS membrane. The observed yield of patterned lines remaining on the OTS-modified substrate ranges between 60% and 70% for our PZT samples.

The lateral shrinkage during the heat treatment also leads to the formation of small voids along the interface between the silicon substrate and the PZT, which can be seen in Fig. 4(b). These voids appear in the silicon oxide interface layer that grows during heat treatment. It is unclear what the exact mechanism is for this development, but it appears that the reaction of the sol-gel components with the substrate surface in this interface layer plays a role in the formation of the voids. Since in device applications PZT will not be placed on silicon directly but on a conductive electrode instead, we opted not to investigate the details of this reaction. The nature of the problem is changed when allowing the thin film greater freedom to relax laterally by coating the silicon substrate with OTS. The OTS reduces the extent of the chemical reactions between the sol-gel components with the substrate while reducing the friction at the interface. As shown in Fig. 5, the reduced interfacial binding can result in regions of delamination consolidated at the interior region of the patterned line in the place of the smaller voids observed with the uncoated substrates. Unfortunately, this phenomenon may prove problematic for ensuring good contacts between the patterned thin film and the substrate for electrical and mechanical properties in potential applications.

Typically, PZT is deposited on a conductive surface to facilitate electrode deposition for device applications. These surfaces can be either metallic, such as electron beam evaporated Pt, or conductive oxide layers, such as $\text{La}(\text{Sr}_{0.5}\text{Co}_{0.5})\text{O}_3$ to suppress the loss of switchable polarization and device fatigue.³⁴ To demonstrate the self-aligning capability of μCM in a multiple-step process, patterns of PZT on top of patterned platinum electrodes are shown in Fig. 6. PZT sol-gel wets Pt with great

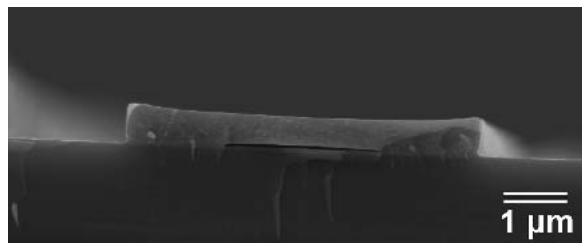


FIG. 5. Close-up SEM image of PZT patterned in OTS-treated rectangular channels showing delamination along the central portion of the PZT thin film-silicon interface.

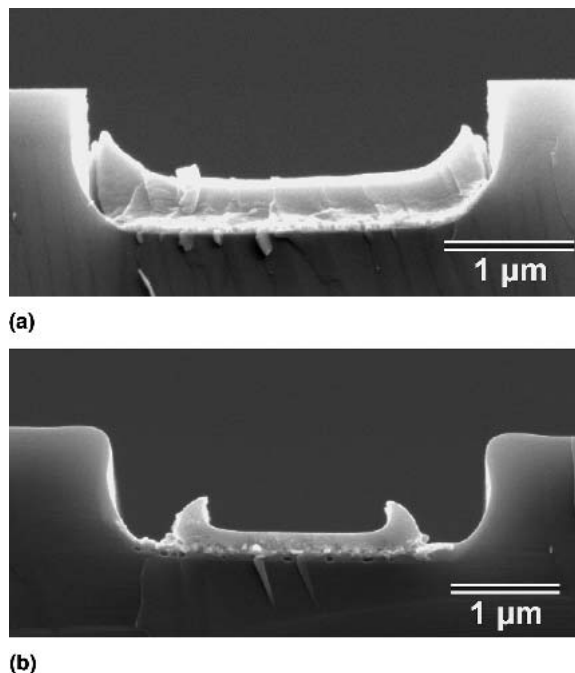


FIG. 6. SEM images of PZT patterned by μCM in rectangular channels formed by RIE with Pt deposited on the bottom surface (a) after drying and (b) after heat treatment.

affinity and forms a very strong bond with the electrode material during heat treatment due to the formation of a metastable Pt_3Pb intermetallic phase at the interface.^{35,36} As a result, the amount of curling at the edges of the patterned lines when using rectangular channels with Pt coated on the bottom is greatly reduced, and the PZT lines stay better pinned to the corners of the channel. However, the magnitude of the topographical defects at the edge is on the same order of magnitude as the thickness of the sintered line and still poses significant obstacles in a manufacturing process.

To replicate the results achieved with the OTS-modified silicon sidewalls, we attempted to deposit self-assembled monolayers on the Pt-coated bottom in an attempt to mitigate this problem. We tested both pentadecanenitrile and octadecanethiol, as these oligomers had single carbon chain backbone structures similar in length to that of OTS with head groups that bind to metals such as Pt. As shown in Fig. 7, the thin films show uniform lateral and vertical shrinkage during the initial drying step. Unfortunately, the presence of the SAM on the platinum layer on the bottom of the thin film dramatically reduces the binding affinity of the substrate to the thin film and the edges of the patterned lines curl and buckle. Large regions of the pattern thin film completely debond from the substrate; the resulting yield of patterned PZT lines bound to the modified metal-coated channels ranges between 40% and 60%. One potential explanation for this result is that presence of the SAM

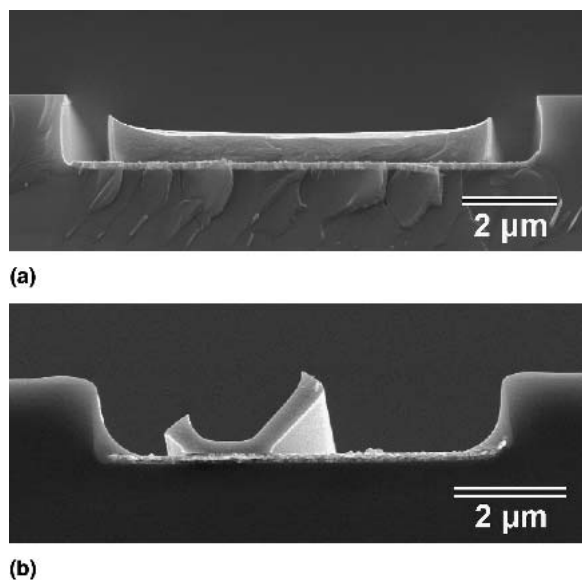


FIG. 7. SEM images of PZT patterned by μ CM in rectangular channels formed by RIE with Pt deposited on the bottom surface with SAM treatment: (a) after drying using octadecanethiol and (b) after heat treatment using pentadecanenitrile.

blocks the growth of the interfacial Pt_3Pb intermetallic phase leading to delamination. Another explanation is the growth of the silicon dioxide layer during heat treatment on the all-silicon channels plays a larger role than originally anticipated in counteracting the delaminating effects of the pyrolyzed SAM during heat treatment. At this time, the self-aligning electrode feature of μ CM is suitable only for patterned thin film applications that do not require high-temperature heat treatment. Further optimization in the choice of SAM tailored to control the binding affinity of the sol-gel to the electrode surface should lead to the production of patterns with rectangular cross sections. Finally, it must be noted that this self-aligning capability is limited only to the deposition of patterns directly on top of other layers; the deposition of layers of arbitrary orientation and shape relative to the thin film still requires photolithography-based procedures or other soft lithography approaches.

To this point, this work has focused on forming the channel patterns for μ CM by etching trenches into the substrate. This is not necessarily a requirement to use the μ CM procedure. A pattern of raised features can be patterned on top of the substrate to form the network of channels for μ CM. Photolithography approaches need not be used, and soft lithography techniques such as MIMIC could be used to define these raised features. Due to incompatibility of the PZT sol-gel with many photoresists and the requirement for heat treatment to 600 °C, we could not demonstrate this feature with our sol-gel and a polymer-based system. Instead we sputter-coated a thick layer of chromium on the surface and used photolithography and wet-chemical etching with

commercial Cr-7 etchant to define the channels. The channels were then filled with the PZT sol-gel by μ CM. The resulting sintered lines are shown in Fig. 8. The sintered PZT lines do not dissolve when Cr-7 is used to dissolve the Cr channels to leave behind a flat substrate; however, some residual Cr intermediaries are formed by reaction with the silicon surface during the heat treatment step and are left behind on the surface. Figure 8(d) shows the roughness of the edges of the PZT lines and the residue left after the Cr wet chemical etch. The edge roughness of the PZT results directly from the poor resolution of the process used to pattern the Cr lines with the Cr-7 wet chemical etch. While Cr and Cr-7 would not be

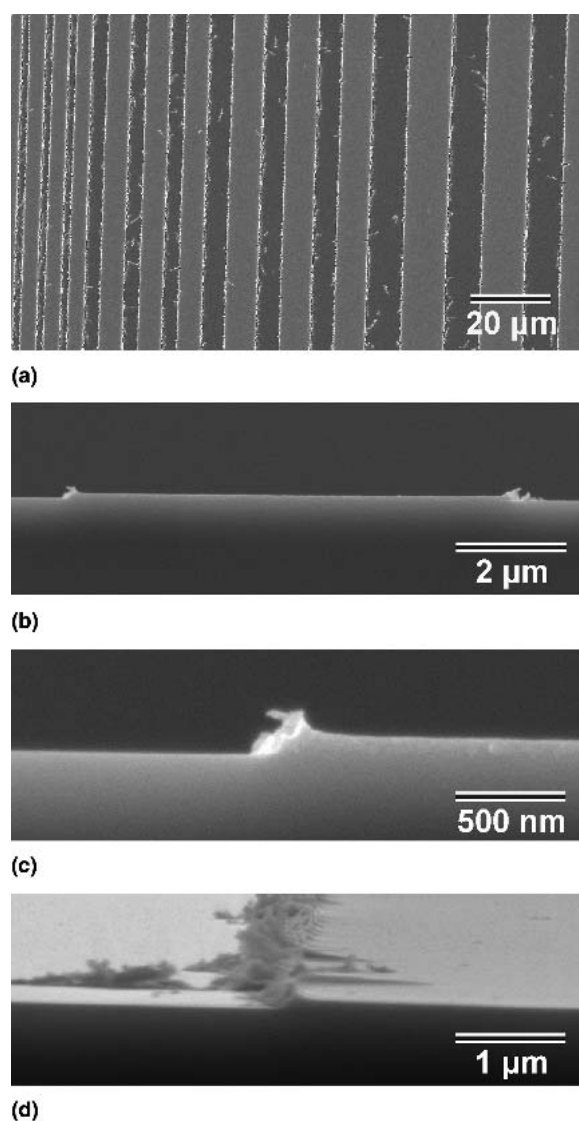


FIG. 8. SEM images of PZT patterned by μ CM using a network of 1- μ m-thick Cr channels deposited on Si after Cr removal: (a) top-view image of patterned PZT lines of various widths, (b) cross-section image of PZT line with close-up (c), and (d) cross-section image taken at a different angle showing roughness of PZT edges resulting from roughness and residue from Cr.

the ideal choice for patterning PZT in true applications, this work illustrates proof of the concept.

IV. CONCLUSIONS

μ CM has the potential to become a useful technique to complement MIMIC for the low cost patterning of thin films derived from liquid precursor solutions. When the surfaces are carefully tailored to decrease the wetting affinity of the sol-gel to the channel walls, three-dimensional structures can be patterned that better replicate the original shape of the mold than with MIMIC. This is due to the elimination of the two dimensional evaporation profile that exists in the PDMS mold in MIMIC where the rate of drying is accelerated at the corners of the mold, leading to the double-peak topographical profile. Unfortunately, when the surfaces of the channels in μ CM are not tailored with SAMs to control the wetting properties, the wetting of the sol-gel to the sidewalls leads to a build-up of material at the sides of the channels that is pulled inward by shrinkage forces during heat treatment. This leads to curling of the patterned lines along the edges.

One advantage of μ CM in manufacturing is its self-aligning ability for patterning multiple layers in a hierarchical structure. We have demonstrated the ability to fabricate the PZT lines with a patterned bottom electrode by depositing a Pt layer at the bottom of the channels by lift-off with the photoresist used to pattern the channels. Similarly multiple layers of different materials could easily be deposited sequentially by μ CM, unlike with other the soft lithography methods, which would require optical microscopes and manipulators to align new molds for each layer. Unfortunately, this feature is restricted to materials that do not require high-temperature heat treatment of the patterned thin film as the use of SAMs does not mitigate the curling phenomenon.

μ CM is not limited to simply etching channels into substrates by photolithography-based means, as the only requirement is a network of channels formed by a pattern of raised features consisting of a compatible material to liquid precursor solution. Further study with surface-modification techniques and new materials is required to overcome the curling limitations and material restrictions currently preventing μ CM from becoming a technique ready to be fully exploited for the low-cost patterning for materials derived from a liquid precursor.

ACKNOWLEDGMENTS

We wish to thank M. Apel-Paz and T.K. Vanderlick at Princeton University for use of their goniometer. The work was jointly supported by NASA Grant No. NAG-2-1475 and by the NASA University Research, Engineering, and Technology Institute on BioInspired Materials (BIMat) under Award No. NCC-1-02037.

REFERENCES

1. Y. Xia and G.M. Whitesides: Soft Lithography. *Ann. Rev. Mater. Sci.* **28**, 153 (1998).
2. X-M. Zhao, Y. Xia, and G.M. Whitesides: Fabrication of three-dimensional micro-structures: Microtransfer molding. *Adv. Mater.* **8**, 837 (1996).
3. J.H. Kim, F.F. Lange, and C-I. Cheon: Epitaxial growth of patterned SrBi₂Ta₂O₉ lines by channel stamping. *J. Mater. Res.* **14**, 1194 (1999).
4. P.M. Moran and F.F. Lange: Microscale lithography via channel stamping: Relationships between capillarity, channel filling, and debonding. *Appl. Phys. Lett.* **74**, 1332 (1999).
5. E. Kim, Y. Xia, and G.M. Whitesides: Polymer microstructures formed by molding in capillaries. *Nature* **376**, 581 (1995).
6. Y. Xia, E. Kim, and G.M. Whitesides: Micromolding of polymers in capillaries: Applications in microfabrication. *Chem. Mater.* **8**, 1588 (1996).
7. E. Kim, Y. Xia, and G.M. Whitesides: Micromolding in capillaries: Applications in materials science. *J. Am. Chem. Soc.* **118**, 5722 (1996).
8. M. Trau, N. Yao, E. Kim, Y. Xia, G.M. Whitesides, and I.A. Aksay: Microscopic patterning of orientated mesoscopic silica through guided growth. *Nature* **390**, 674 (1997).
9. P. Yang, T. Deng, D. Zhao, P. Feng, D. Pine, B.F. Chmelka, G.M. Whitesides, and G.D. Stucky: Hierarchically ordered oxides. *Science* **282**, 2244 (1998).
10. W.S. Beh, Y. Xia, and D. Qin: Formation of patterned microstructures of polycrystalline ceramics from precursor polymers using micromolding in capillaries. *J. Mater. Res.* **14**, 3995 (1999).
11. S. Seraji, Y. Wu, N.E. Jewell-Larson, M.J. Forbess, S.J. Limmer, T.P. Chou, and G. Cao: Patterned microstructure of sol-gel derived complex oxides using soft lithography. *Adv. Mater.* **12**, 1421 (2000).
12. J.S. Vartuli, M. Özenbaş, C-M. Chun, M. Trau, and I.A. Aksay: Micropatterned lead zirconium titanate thin films. *J. Mater. Res.* **18**, 1259 (2003).
13. C.R. Martin and I.A. Aksay: Topographical evolution of lead zirconate titanate (PZT) thin films patterned by micromolding in capillaries. *J. Phys. Chem. B* **107**, 4261 (2003).
14. M. Heule and L.J. Gauckler: Gas sensors fabricated from ceramic suspensions by micromolding in capillaries. *Adv. Mater.* **13**, 1790 (2001).
15. C. Marzolin, S.P. Smith, M. Prentiss, and G.M. Whitesides: Fabrication of glass microstructures by micro-molding of sol-gel precursors. *Adv. Mater.* **10**, 571 (1998).
16. A. Matsuda, Y. Matsuno, M. Tatsumisago, and T. Minami: Fine patterning and characterization of gel films derived from methyltriethoxysilane and tetraethoxysilane. *J. Am. Ceram. Soc.* **81**, 2849 (1998).
17. O.J.A. Schueller, G.M. Whitesides, J.A. Rogers, M. Meier, and A. Dodabalapur: Fabrication of photonic crystal lasers by nano-molding of sol-gel glasses. *Appl. Opt.* **38**, 5799 (1999).
18. C.A. Bulthaup, E.J. Wilhelm, B.N. Hubert, B.A. Ridley, and J.M. Jacobson: All-additive fabrication of inorganic logic elements by liquid embossing. *Appl. Phys. Lett.* **79**, 1525 (2001).
19. A. Kumar and G.M. Whitesides: Features of gold having micrometer to centimeter dimensions can be formed through a combination of stamping with an elastomeric stamp and an alkanethiol 'ink' followed by chemical etching. *Appl. Phys. Lett.* **63**, 2002 (1993).
20. A. Kumar, H.A. Biebuyck, and G.M. Whitesides: Patterning self-assembled monolayers—Applications in materials science. *Langmuir* **10**, 1498 (1994).
21. N.L. Jeon, P.G. Clem, R.G. Nuzzo, and D.A. Payne: Patterning of

- dielectric oxide thin-layers by microcontact printing of self-assembled monolayers. *J. Mater. Res.* **10**, 2996 (1995).
22. N.L. Jeon, P.G. Clem, D.A. Payne, and R.G. Nuzzo: A monolayer-based lift-off process for patterning chemical vapor deposition copper thin films. *Langmuir* **12**, 5350 (1996).
 23. P.G. Clem, N-L. Jeon, R.G. Nuzzo, and D.A. Payne: Monolayer-mediated deposition of tantalum(V) oxide thin film structures from solution precursors. *J. Am. Ceram. Soc.* **80**, 2821 (1997).
 24. N.L. Jeon, P. Clem, D.Y. Jung, W. Lin, G.S. Girolami, D.A. Payne, and R.G. Nuzzo: Additive fabrication of integrated ferroelectric thin-film capacitors using self-assembled organic thin-film templates. *Adv. Mater.* **9**, 891 (1997).
 25. D.A. Payne and P.G. Clem: Monolayer-mediated patterning of integrated electroceramics. *J. Electroceram.* **3**, 163 (1999).
 26. Y.K. Hwang, S.Y. Woo, J.H. Lee, D-Y. Jung, and Y-U. Kwon: Micropatterned CdS thin films by selective solution deposition using microcontact printing techniques. *Chem. Mater.* **12**, 2059 (2000).
 27. M. Bartz, A. Terfort, W. Knoll, and W. Tremel: Stamping of monomeric SAMs as a route to structured crystallization templates: Patterned titania films. *Chem. Eur. J.* **6**, 4149 (2000).
 28. H. Shin, J.U. Jeon, Y.E. Pak, H. Im, and E.S. Kim: Formation and characterization of crystalline iron oxide films on self-assembled organic monolayers and their in situ patterning. *J. Mater. Res.* **16**, 564 (2001).
 29. C.R. Martin and I.A. Aksay: Submicrometer-scale patterning of ceramic thin films. *J. Electroceramics* **12**, 53 (2004).
 30. C.R. Aksay: Low-cost patterning of ceramic thin films, in *Electroceramic-Based MEMS: Fabrication-Technology and Applications*, edited by N. Setter (Springer Science+Business Media, New York, 2005), p. 387.
 31. A. Folch and M.A. Schmidt: Wafer-level in-registry microstamping. *J. Microelectromech. Syst.* **8**, 85 (1999).
 32. G. Yi, Z. Wu, and M. Sayer: Preparation of Pb(Zr,Ti)O₃ thin films by sol gel processing: Electrical, optical, and electro-optic properties. *J. Appl. Phys.* **64**, 2717 (1988).
 33. H.J. Shin, Y.H. Wang, U. Sampathkumaran, M.R. DeGuire, A.H. Heuer, and C.N. Sukenik: Pyrolysis of self-assembled organic monolayers on oxide substrates. *J. Mater. Res.* **14**, 2116 (1999).
 34. C.S. Ganpule, A. Stanishevsky, Q. Su, S. Aggarwal, J. Melngailis, E. Williams, and R. Ramesh: Scaling of ferroelectric properties in thin films. *Appl. Phys. Lett.* **75**, 409 (1999).
 35. Z. Huang, Q. Zhang, and R.W. Whatmore: Low temperature crystallization of lead zirconate titanate thin films by a sol-gel method. *J. Appl. Phys.* **85**, 7355 (1999).
 36. Z. Huang, Q. Zhang, and R.W. Whatmore: Structural development in the early stages of annealing of sol-gel prepared lead zirconate titanate thin films. *J. Appl. Phys.* **86**, 1662 (1999).